THE JOURNAL OF BIOLOGICAL CHEMISTRY
Vol. 277, No. 38, Issue of September 20, pp. 34902–34908, 2002
Printed in U.S.A.

Coordinated Folding and Association of the LIN-2, -7 (L27) Domain

AN OBLIGATE HETERODIMERIZATION MODULE INVOLVED IN ASSEMBLY OF SIGNALING AND CELL POLARITY COMPLEXES*

Received for publication, June 12, 2002
Published, JBC Papers in Press, July 10, 2002, DOI 10.1074/jbc.M205856200

Baruch Z. Harris‡§, Shivkumar Venkatasubrahmanyam‡§, and Wendell A. Lim¶‖

From the ‡Program in Biological Sciences and the ¶Department of Cellular and Molecular Pharmacology, University of California, San Francisco, California 94143-0450

LIN-2, -7 (L27) homology domains are putative protein-protein interaction modules found in several scaffold proteins involved in the assembly of polarized cell-signaling structures. These specific interaction pairs are well conserved across metazoan species, from worms to man. We have expressed and purified L27 domains from multiple species and find that certain domains from proteins such as *Caenorhabditis elegans* LIN-2 and LIN-7 can specifically heterodimerize. Biophysical analysis of interacting L27 domains demonstrates that the domains interact with a 1:1 stoichiometry. Circular dichroism studies reveal that the domains appear to function as an obligate heterodimer; individually the domains are largely unfolded, but when associated they show a significant increase in helicity, as well as a cooperative unfolding transition. These novel obligate interacting pairs are likely to play a key role in regulating the organization of signaling proteins at polarized cell structures.

In multicellular organisms, many cells are highly polarized to allow for specific cell-cell communication. An essential feature of polarized cells is the organization of signaling proteins into distinct membrane domains (1, 2). For example, both neurons and epithelial cells actively maintain regions of the cell surface to which receptors, downstream signaling molecules, and structural proteins are selectively targeted. To accomplish this function, cells often use multivalent scaffolding proteins that bring together diverse signaling molecules into supramolecular complexes. These scaffolding proteins generally have multiple protein-protein recognition modules that play an important role in the assembly and dynamic regulation of signaling complexes (3).

Multivalent scaffolding molecules assemble such structures by participating in two general classes of binding interactions. First, they bind to non-scaffolding molecules, usually signaling proteins such as receptors or downstream effectors. These interactions are often mediated by well characterized modular recognition domains, including PSD-95·Dlg·ZO-1 homology (PDZ)[1] domains (4), which bind target proteins through short peptide motifs. Second, scaffold proteins can form higher order multiprotein networks through homo- or hetero-oligomerization with other scaffolding molecules (5). Far less is understood about the mechanism of such oligomerization interactions, although they are also essential for proper complex assembly.

A notable example of a multiprotein scaffold network is the LIN-2/LIN-7/LIN-10 heterotrimeric complex (6), which is responsible for receptor targeting in polarized cells in a variety of metazoan organisms (7–17). In this heterotrimeric complex, each scaffold protein has one or more PDZ domains that specifically interact with other partner/signaling proteins (Fig. 1). In addition, the three proteins interact with one another independently of their PDZ domains. LIN-2 homologs are members of a larger family of scaffold proteins referred to as membrane-associated guanylate kinases (MAGUKs), which contain PDZ, SH3, and guanylate kinase-like domains (3, 7); LIN-7 and LIN-10 comprise distinct families of scaffolding molecules.

The LIN-2·LIN-7·LIN-10 complex was first identified in *Caenorhabditis elegans*. Mutation of these proteins leads to aberrant localization of the epidermal growth factor receptor-like tyrosine kinase receptor LET-23 in vulval precursor epithelial cells; instead of being properly targeted to the basolateral surface where it is positioned to receive its extracellular signal, LET-23 is found at the apical membrane. Mislocalization of the receptor leads to a loss in LET-23-dependent signaling and defects in vulval induction (8–11). The LIN-2, LIN-7, and LIN-10 proteins have been found to form a trimeric complex. In addition, the PDZ domain from LIN-7 interacts with the C terminus of LET-23 (9). Although the LIN-2·LIN-7·LIN-10 complex is probably required simply for localization of LET-23 and therefore only indirectly involved in signaling, loss of any member of the complex has a similar phenotype with respect to vulval induction as loss of the receptor (10). LIN-10 has also been observed to play a crucial role in neuronal receptor targeting in *C. elegans* (12), suggesting that the LIN-2, LIN-7, and LIN-10 proteins function in polarized targeting in a variety of cell types.

Homologs of LIN-2, LIN-7, and LIN-10 have also been identified in mammals; they are called CASK/PALS, VELI/MALS, and MINT/X11, respectively (13–20). These proteins have been observed in most neuronal and epithelial cell types and form a variety of dimeric or trimeric complexes (13, 21–25). In these complexes, PDZ domains in each of the scaffold proteins are used to bind various signaling or transport proteins (9, 12, 13, 21, 24, 26). In mammalian dendrites, the PDZ domain from VELI/MALS binds the C-terminal tail of the *N*-methyl-D-aspartate receptor subunit NR2B in a fashion analogous to the binding of the LIN-7 PDZ domain to the C-terminal tail of LET-23. In addition, the PDZ domain from MINT1/X11α binds to the kinesin superfamily motor protein KIF17. The CASK/

* This research was supported by grants from the National Institutes of Health and the David and Lucille Packard Foundation (to W. A. L.). The costs of publication of this article were defrayed in part by the payment of page charges. This article must therefore be hereby marked "*advertisement*" in accordance with 18 U.S.C. Section 1734 solely to indicate this fact.

§ Howard Hughes Predoctoral Fellow.
‖ To whom correspondence should be addressed. Tel.: 415-502-8080; Fax: 415-502-8644; E-mail: wlim@itsa.ucsf.edu.

[1] The abbreviations used are: PDZ, PSD-95·Dlg·ZO-1 homology; GST, glutathione *S*-transferase; NTA, nitrilotriacetic acid; DTT, dithiothreitol; PBS, phosphate-buffered saline.

PALS protein tethers the other two scaffold proteins together, just as LIN-2 tethers LIN-7 and LIN-10 (24). It has been proposed that the entire heterotrimeric complex is involved in transport of vesicles containing *N*-methyl-D-aspartate receptors to the postsynaptic density (24). More recent evidence indicates an important role for mammalian LIN-2·LIN-7·LIN-10 proteins in receptor localization and endosomal sorting in epithelial cells (25, 27).

Little is known about the interactions used to assemble the trimeric scaffold network. Recently, Doerks *et al.* (28) identified regions of significant sequence homology within many members of the LIN-2 and LIN-7 family, which they termed "L27" domains, for LIN-2/LIN-7 dimerization. These putative domains are all within regions of LIN-2 and LIN-7 (or homologs) that have previously been implicated in association of the two scaffold proteins (13, 22, 23, 27). Moreover, the L27 homology region appears to be the minimal region required for LIN-2/LIN-7 association. Therefore, the L27 domain is postulated to be a protein-protein interaction module critical for the assembly of this higher order scaffolding structure (29, 30).

Here we report the expression, purification, and biochemical characterization of several L27 domains from both *C. elegans* and mammals. We observe a specific interaction between domains from the LIN-2/CASK family and domains from the LIN-7/VELI/MALS family. This interaction functions both within species and across species. We also observe that L27 domains assemble into a 1:1 heterodimer with binding affinities in the low micromolar range. Finally, we find that isolated L27 domains appear to be relatively unstructured but adopt a stable folded structure upon heterodimeric association. Thus, the domains act as obligate heterodimers.

EXPERIMENTAL PROCEDURES

L27 Domain Cloning and Expression—Using the L27 sequence profile of Doerks *et al*. (28), we identified putative L27 domains in the following proteins; from *C. elegans*, LIN-2a and LIN-7 (8, 10); from *Rattus norvegicus*, the LIN-7 homolog LIN-7-BA (16); and from *Homo sapiens*, the LIN-2 homolog CASK (14). Here we employ the following nomenclature to describe each L27 domain: the abbreviated name of the species of origin (C.e., R.n., or H.s.), followed by the name of the orthologous protein from *C. elegans* (LIN-7, LIN-2) and N or C denoting N- or C- terminal, for cases in which a protein has two domains. For example, the *H. sapiens* C-terminal CASK L27 domain is denoted by "H.s. LIN-2C."

DNA regions encoding the putative L27 domains were cloned by PCR from cDNA libraries and expressed as fusion proteins to both N-terminal hexahistidine (His_6) and glutathione *S*-transferase (GST) tags for purification and biochemical characterization. Regions cloned comprised the following amino acids: *C. elegans* LIN-7 115–180 (C.e. LIN-7), *C. elegans* LIN-2a 363–430 (C.e. LIN-2N) and 423–487 (C.e. LIN-2C), *R. norvegicus* LIN-7-BA 10–75 (R.n. LIN-7), and *H. sapiens* CASK 335–401 (H.s. LIN-2N) and 394–460 (H.s. LIN-2C). The cloned regions include five extra amino acids added to both the N and C termini of the putative homology regions as a safety margin to allow for expression of stable and soluble domains. PCR products were ligated into expression vectors pBH4 (31) for His_6 fusions or pGEX4T1 for glutathione *S*-transferase fusions. All constructs were verified by DNA sequencing on both strands.

Protein constructs were expressed in the *E. coli* strain BL21 pLYS-S (Invitrogen). Cultures were grown at 25 °C because of increased protein solubility at this temperature and induced with 1 mM isopropyl-1-thio-β-D-galactopyranoside. After induction for 6 h, cultures were harvested by centrifugation, resuspended in ~25 ml of 50 mM Tris-Cl, pH 7.5, 300 mM NaCl per original liter of culture, and subjected to freeze-thaw treatment. Cell suspensions were lysed by sonication and cleared by centrifugation at 20,000 × *g*.

Three forms of recombinant proteins were used in this study. First, crude fractionated lysates containing His_6 fusions for use as "prey" in GST-pulldown assays were prepared by expression as described above, followed by incubation with Ni^{2+}-NTA Superflow™ resin (Qiagen) for ~30 min. The resin was extensively washed with 50 mM Tris-Cl, pH 7.5, 300 mM NaCl, and bound protein eluted with 250 mM imidazole in 50 mM sodium phosphate buffer, 300 mM NaCl, pH 8.0 to >50% purity. His_6 fusion constructs purified in this manner were then dialyzed extensively against 20 mM HEPES pH 7.0, 1 mM DTT and used immediately for pulldown assays. Second, GST fusions for use as "bait" in GST-pulldown assays were incubated with glutathione-agarose resin (Sigma) for 30 min at 4 °C followed by extensive washing in 1× phosphate-buffered saline (PBS), 2 mM DTT. Third, untagged proteins used in quantitative biochemical experiments were generated by thrombin cleavage of the GST fusion proteins. Cleavage was performed by adding thrombin (Hematologic Technologies, Inc.) at a concentration of ~6.5 μg/ml to a slurry of fusion protein bound to glutathione-agarose. Cleavage reactions were rotated overnight at 4 °C, and cleaved protein was separated from the resin by filtration. Cleaved L27 domains were further purified by ion exchange chromatography in 20 mM Tris-Cl, 1 mM DTT, 0–500 mM NaCl, pH 7.0 on an HR10/10 Source Q Sepharose column (Amersham Biosciences) to >99% purity and stored in 20 mM HEPES pH 7.0, 1 mM DTT.

GST Pulldowns—GST fusions of L27 domains for use as bait were expressed and purified as described above. 25 μl of GST-L27 domain slurry was incubated with ~150 μl of eluted His_6 L27 domain in a final buffer of 20 mM HEPES pH 7.0, 10 mM NaCl, 2 mM DTT for 30 min, followed by three washes with 1× PBS containing 0.1% Triton X-100, then two washes in 1× PBS with no detergent. Bound proteins were eluted from the resin in 2× SDS sample buffer and subsequently visualized with SDS-PAGE followed by Western blotting with anti-hexahistidine antibodies.

Fluorescence Perturbation Binding Assays—Purified H.s. LIN-2C and C.e. LIN-2C domains were conjugated to a fluorescent dansyl moiety by covalent linkage to endogenous cysteines (corresponding to residues 464 and 473 in *C. elegans* LIN-2a and residue 412 in *H. sapiens* CASK). 100 μM protein was incubated with 2 mM dansyl iodoacetamide (Molecular Probes) in 20 mM HEPES pH 7.0 overnight at 4 °C. Labeled proteins were purified over a PD-10 gel filtration column (Amersham Biosciences) and redialyzed into storage buffer (20 mM HEPES pH 7.0, 1 mM DTT). Fluorescence was assayed in a 1 × 1 cm stirred cell cuvette in a buffer containing 50 mM HEPES pH 7.5, 50 mM NaCl at 20 °C using a Photon Technology Inc. Quantum Master fluorometer. Changes in fluorescence intensity were recorded, and data were fit to a bimolecular binding equation using Profit 5.1.0 (Quantum Soft). For conditions in which [L]≫[P], we fit the data as described previously (32). For conditions in which [L] approached [P], we used the analysis described by Nguyen *et al.* (33). All binding experiments were repeated 3–4 times. Binding of dansylated 2C domains to C.e. LIN-7 was verified independently by GST pulldown assay and showed no detectable difference from unlabeled 2C domains. The R.n. LIN-7 L27 domain was too insoluble to purify in quantities sufficient to perform binding assays. To confirm that the dansyl modifications did not alter binding affinity, we also performed competition binding assays (32) in which the unlabeled proteins were used to compete off identical labeled proteins. Quantitative analysis of these data revealed no effect of the label (data not shown).

Analytical Ultracentrifugation—Analytical ultracentrifugation experiments were performed on a Beckman Optima XL-A analytical ultracentrifuge with dual beam detection at 280 or 504 nm and with an An-60Ti rotor having sectored cells composed of sapphire- and carbon-impregnated Epon. Data were parsed with Win ReEdit version 0.999.0023 and analyzed with WinNonLin version 1.060 (David Yphantis, University of Connecticut) and Profit 5.1.0 (Quantum Soft). Single species experiments were fit to Equation 1.

$$A_{TOT} = A_0 e^{\sigma\left(\frac{r^2}{2} - \frac{r_0^2}{2}\right)} \quad \text{(Eq. 1)}$$

In Equation 1 A_{TOT} is the total absorbance measured by the spectrophotometer, A_0 is the absorbance constant, r is the radius, and r_0 is the minimum radius (*i.e.* radius of meniscus). σ denotes the following expression shown as Equation 2.

$$\sigma = \frac{M\omega^2(1 - \bar{v}\rho)}{RT} \quad \text{(Eq. 2)}$$

In Equation 2 M is the molecular mass (g/mol), ω is the angular velocity of the rotor (rads/s), $\bar{v}$ is the partial specific volume (cm^3/g), ρ is the solvent density, R is the gas constant, and T is the absolute temperature in degrees Kelvin. Two-species data were fit using Equation 3.

$$A_{TOT} = A_1 e^{\sigma_1\left(\frac{r^2}{2} - \frac{r_0^2}{2}\right)} + A_2 e^{\sigma_2\left(\frac{r^2}{2} - \frac{r_0^2}{2}\right)} \quad \text{(Eq. 3)}$$

In Equation 3 variables are defined as above, and A_{TOT} is treated as the sum of two distributions; A_1 and σ_1 correspond to monomer values, and

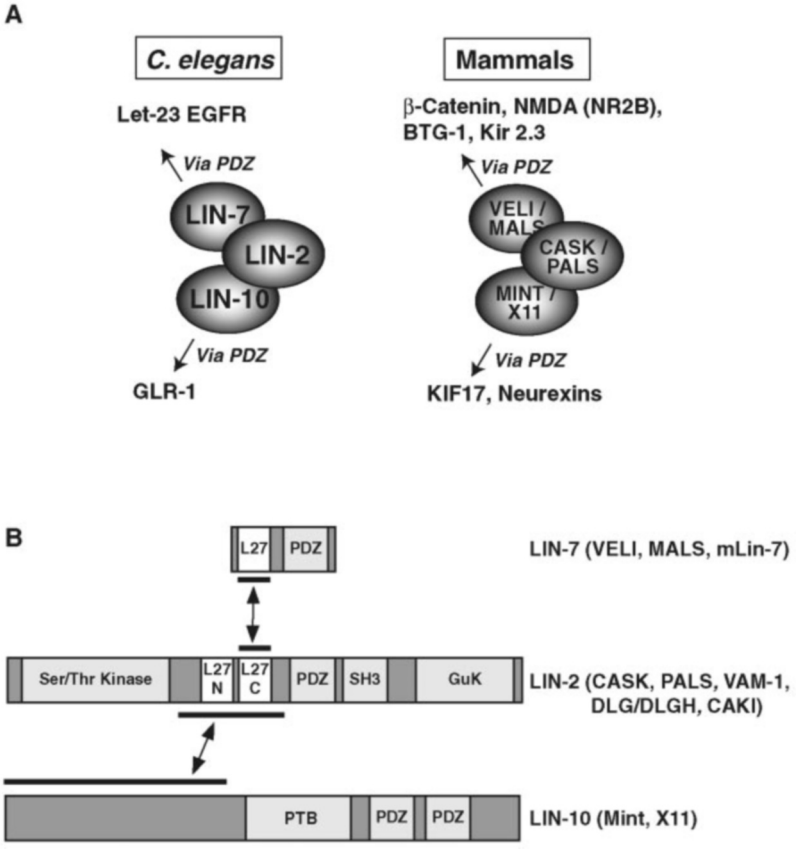

FIG. 1. **Organization and assembly of L27 domain containing scaffolds.** *A*, representation of the LIN-2·LIN-7·LIN-10 complex in *C. elegans* (*left*) and mammals (*right*). LIN-2 binds both LIN-7 and LIN-10 to form a heterotrimeric complex. Ligands that bind the PDZ domains of LIN-7 and LIN-10 are indicated above and below. *B*, domain organization of LIN-2, LIN-7, and LIN-10. L27 homology regions (28) are *highlighted* in *white*. Other known domains (*SH3*, Src homology 3; *PDZ*, PSD95·Dlg·ZO-1 homology; *GuK*, guanylate kinase-like; *PTB*, phosphotyrosine binding) are shown in *gray*. Previously delineated minimal interaction regions between LIN-2 and LIN-7 or LIN-10 are indicated with *black bars* (22, 23, 29). Names of mammalian orthologs of LIN-7, LIN-2, and LIN-10 proteins are indicated in *parentheses*. The relative scale depicted in this panel is from primary amino acid sequences of LIN-7BA (*R. norvegicus*), mLin2·CASK (*H. sapiens*), and X11α (*H. sapiens*) (39, 43). Other L27-containing proteins have the same qualitative domain organization but are not necessarily to scale with this diagram.

A_2 and σ_2 correspond to heterodimer values. Experiments with L27 monomers alone were checked using WinNonLin; data fit in all cases to a single-species model with monomeric molecular weight, and no higher aggregation states could be fit. Analysis of heterodimers with one labeled species was performed as described (34, 35). Proteins used for analytical ultracentrifugation experiments were purified as described above or specifically labeled as follows: purified H.s. LIN-2C and C.e. LIN-2C domains were conjugated to a fluorescent BODIPY moiety by covalent linkage to endogenous cysteines (corresponding to residues 464 and 473 in *C. elegans* Lin-2a and residue 412 in *H. sapiens* CASK). Labeling was performed by incubating 100 μM protein with 2 mM BODIPY maleimide (Molecular Probes) in 20 mM HEPES pH 7.0 overnight at 4 °C. Labeled proteins were purified over a PD-10 gel filtration column (Amersham Biosciences) and redialyzed into a storage buffer of 20 mM HEPES, 1 mM DTT, pH 7.0. Binding of BODIPY-labeled 2C domains to C.e. LIN-7 was verified independently by GST pulldown assay and showed no detectable difference from unlabeled 2C domains. We were not able to exceed a C.e. LIN-7:LIN-2C ratio of 25:1 as the C.e. LIN-7 monomer shows significant non-ideal behavior at concentrations $\geq$25 μM, which leads to a decrease in the apparent molecular weight of either heterodimer.

Circular Dichroism—Circular dichroism spectroscopy was performed using either an AVIV model 62DS or JASCO 715 spectrapolarimeter. All scans were performed with untagged, purified proteins in a 0.1-cm quartz cuvette in 20 mM HEPES pH 7.5; data for scans were collected at 1 nm intervals, with 1 s averaging time per data point and a total of 10 repeats per scan. Temperature denaturation studies were performed in 0.1-, 0.5-, or 1.0-cm path length quartz cuvettes with 50 mM sodium phosphate buffer, pH 7.5, 10 mM NaCl. Data for melts was collected at 1 °C intervals, with 60 s averaging time and 60 s of equilibration time per data point. Proteins subjected to temperature melts were scanned in every case (200–300 nm) before and after each melt to verify reversibility.

RESULTS AND DISCUSSION

Selected L27 Domains Are Capable of Specific Heterodimerization—To assess the binding capacity of putative L27 domains, we performed GST-pulldown assays, cross-testing all possible combinations of the six cloned domains (C.e. and R.n. LIN-7, C.e. and H.s. LIN-2N, C.e. and H.s. LIN-2C). In each case, a GST-tagged bait domain was used to pull down a His_6-tagged "prey" domain. As shown in Fig. 2, we identified a specific interaction between LIN-2C and LIN-7 L27 domains. This interaction is conserved across species; both mammalian and *C. elegans* LIN-7 L27 domains are able to bind LIN-2C L27 domains from either species. These data are consistent with previous findings that mammalian LIN-2C domains bind mammalian LIN-7 domains (13, 22, 23, 27, 29). Within this set, we did not identify any binding partners for the LIN-2N L27 domain, although recent studies suggest that this domain may be responsible for interaction with another multidomain scaffolding protein, SAP97 (29). Deletion analysis (data not shown) indicates that the boundaries identified by sequence homology (28) correspond to those of the functional domain, deletion of 5–10 additional amino acids results in loss of binding, whereas the addition of 5–10 residues has no noticeable effect on binding.

Binding Affinity of the LIN-7 and LIN-2C L27 Domains—To quantitatively measure the binding affinity of LIN-2C and LIN-7 L27 domains, we took advantage of the fact that both the C.e. LIN-2C and H.s. LIN-2C domains have cysteine residues, to which we covalently attached a fluorescent dansyl group. Dansyl fluorescence is very sensitive to local environment and often changes significantly in response to protein binding. Binding was assayed by measuring the change in fluorescence with increasing amounts of the C.e. LIN-7 domain.

Results of the fluorescence perturbation binding assay for the C.e. LIN-7:C.e. LIN-2C(dansyl) pair are shown in Fig. 3*A* (*filled circles*). The data could be fit well to a bimolecular binding reaction, with a $K_d = 14 \pm 4$ μM (Fig. 3*A*). Scatchard analysis (Fig. 3*B*) is consistent with a 1:1 stoichiometric ratio. For all cases, we confirmed that the dansyl modification did not perturb the affinity by performing a competition binding assay in which the dansylated probe was competed off by addition of undansylated domain. Fits to these data (not shown) indicate

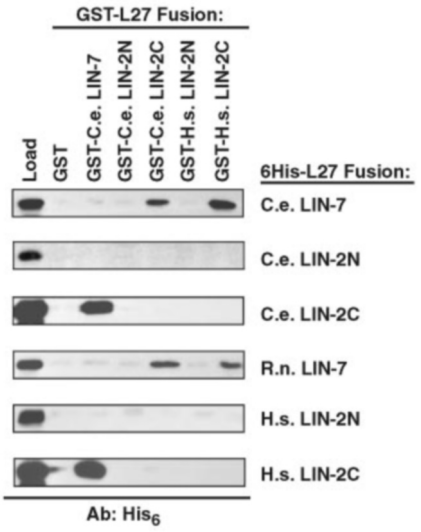

FIG. 2. **Specific heterodimerization of L27 domains.** GST fusions of L27 domains were used as bait to pull down various His_6-tagged prey L27 domains. Prey proteins retained on the resin were subjected to SDS-PAGE and detected by Western blotting with anti-His_6 antibody. Bait constructs used in this interaction array are labeled at the *top*, whereas prey proteins used are labeled on the *side*. Within this matrix of 5 × 6 tested pairs, the only observed interactions involve those between the L27 domain from LIN-7 homologs and the C-terminal L27 (L27C) domain from LIN-2 homologs. Nomenclature denotes species of origin and protein of origin, for example: H.s. LIN-2C is the C-terminal L27 domain from the LIN-2 homolog in *H. sapiens*. In this assay, only minimal L27 domain fusions were used, not full-length proteins.

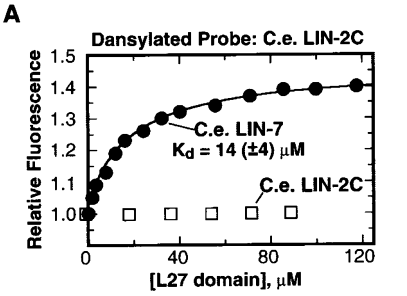

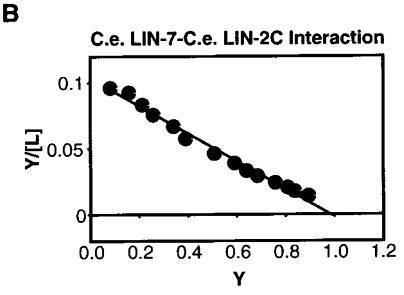

C

Apparent Dissociation Constant (μM)

		Dansylated probe: *C.elegans* LIN-2C	Dansylated probe: *H. sapiens* LIN-2C
C.elegans	LIN-2N	> 200	> 200
	LIN-2C	> 200	> 200
	LIN-7	14	0.09
H. sapiens	LIN-2N	> 200	> 200
	LIN-2C	> 200	> 200

FIG. 3. **Binding affinity of L27 domains.** *A*, binding of C.e. LIN-7 L27 domain to dansylated C.e. LIN-2 (C) L27 domain. Binding was monitored by following change in relative dansyl fluorescence with increasing concentration of the C.e. LIN-7 domain (*filled circles*). K_d value is the average of four independent experiments. For comparison, data observed with a non-binding L27 (H.s. LIN-2C, *squares*) is shown. *B*, Scatchard analysis of binding data shown in *A*. The data shown are for C.e. LIN-7 and C.e. LIN-2C and indicate one binding site for the 7 domain on the 2C domain. The R^2 value for the line is 0.988. *C*, apparent dissociation constants for L27 pairs derived from fluorescence perturbation data.

no significant difference in affinity between the modified and unmodified domains. Addition of up to 50–100 μM of most other purified L27 domains (either 2C or 2N) resulted in no significant change in fluorescence (Fig. 3*A*, *open squares*), confirming the previous GST-pulldown result (Fig. 2) that this heterooligomer interaction is highly specific. The only other L27 domain pair that showed significant binding was the homologous interspecies pair of the H.s. LIN-2C and C.e. LIN-7 domains. Interestingly, this interspecific pair was found to have a K_d = 88 ± 6 nM (Fig. 3*C*) and is therefore ~100-fold higher in affinity than the corresponding intraspecies pair. It is possible that the C.e. LIN-2C domain requires additional regions outside of the domain for high affinity interaction. However, given the high homology between the domains (28% identity, 46% similarity), this explanation seems unlikely. It is more likely that this result represents a real difference in affinity. This finding raises the interesting possibility that the biologically relevant intraspecies pair has evolved to have a suboptimal affinity, which may be more amenable to regulated multiprotein complex assembly.

The LIN-2C and LIN-7 L27 Domains Form a Dimer with 1:1 Stoichiometry—Although LIN-7 and LIN-2 homologs have been shown to bind one another in a wide variety of systems, the precise stoichiometry of the complex is not known. Therefore, the possibility exists that L27 domains form higher order oligomers rather than a simple heterodimer. To further characterize the stoichiometry of the complex and obtain a molecular weight for the interacting pair, we performed equilibrium analytical ultracentrifugation on the tight binding H.s. LIN-2C:C.e. LIN7 L27 pair. H.s. LIN-2C monomer was selectively labeled with a BODIPY fluorophore exhibiting a peak absorbance at 504 nm (at this wavelength nonlabeled monomers have no detectable absorbance). Upon mixing 1 μM labeled H.s. LIN-2C monomer with an excess amount of unlabeled C.e. LIN-7, we were able to follow the equilibrium distribution of the labeled species in an analytical ultracentrifugation experiment. For the C.e. LIN-7:H.s. LIN-2C pair, the fraction bound at these concentrations is very high, and the data are in agreement with a 1:1 heterodimer and inconsistent with alternative higher order oligomers (Fig. 4*A*). Analytical ultracentrifugation of H.s. LIN-2C, C.e. LIN-2C, or C.e. LIN-7 monomers alone gave good fits to a monomer molecular weights over a range of concentrations of ~50–200 μM with no evidence of homodimerization. Thus, we conclude that the LIN-7:LIN-2C L27 domain pair forms a simple heterodimer.

Interacting Domains Show Linked Binding and Folding—We assessed the stability and secondary structure of L27 domains, both as individual proteins and in bound complexes, using circular dichroism spectroscopy. Spectra for L27 monomers show little ellipticity at 222 nm (Fig. 5*A*), characteristic of proteins that have little helical structure. However, we observed a striking increase in ellipticity at 222 nm upon mixing of the monomers; the ellipticity observed is significantly greater than the arithmetic sum of the individual monomer spectra. Specifically, mixed 7 and 2C domains, not other domains alone or in combination, show CD spectra that are characteristic of highly α-helical folded proteins (Fig. 5*A*). We ob-

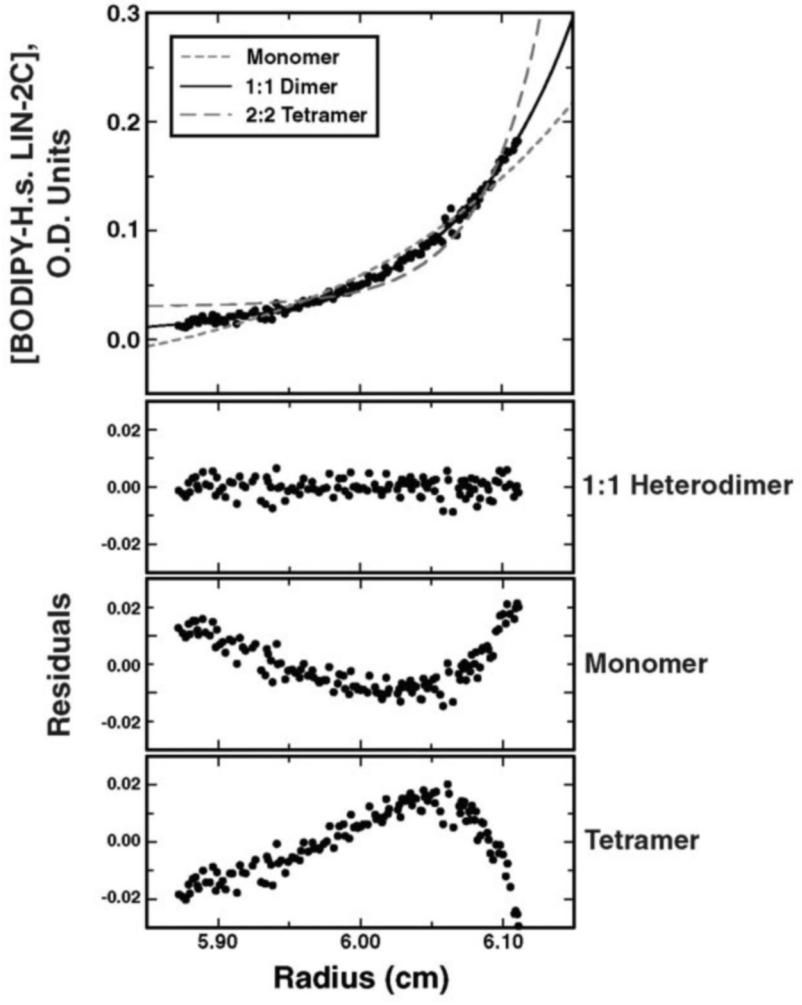

FIG. 4. **Analytical ultracentrifugation of L27 heterodimers reveals a 1:1 stoichiometry.** Fits and residuals for the C.e. LIN-7:H.s. LIN-2C pair at a 25:1 ratio using a single species model with variable σ. The best fit curve with a σ value equivalent to a 1:1 heterodimer is shown as a *solid line*. For comparison, best fit curves with σ equivalent to monomer (*short dashes*) or 2:2 tetramer (*long dashes*) are shown. Residuals for monomer, 1:1 heterodimer, and 2:2 tetramer models are shown below. The experiment shown was performed at 30,000 rpm.

served this for both interacting pairs (C.e. LIN-7:C.e. LIN-2C and C.e. LIN-7:H.s. LIN-2C). The difference spectra indicate the formation of a highly helical structure only upon interaction. However, we do not observe significant changes for nonbinding L27 pairs (Fig. 5*B*).

To further characterize this conformational change upon L27 heterodimerization, we performed temperature-melting experiments on both monomers and heterodimers at 222 nm, a wavelength diagnostic of α-helical secondary structure. We performed these experiments with the high affinity C.e. LIN-7:H.s. LIN-2C pair. As shown in Fig. 5*C*, neither of the individual domains shows a cooperative transition with increasing temperature. The H.s. LIN-2C:C.e. LIN-7 heterodimer, however, displays a clear cooperative unfolding transition. This supports a model in which binding and folding events are linked for the LIN-2C:LIN-7 L27 pair; the individual monomers are largely unfolded but become a stable, helical, folded unit upon association.

If binding and folding events for the LIN-2C:LIN-7 pair are linked, apparent stability of the heterodimer would show a dependence on concentration. To test this, we measured the melting temperature of varying equimolar mixtures of H.s. LIN-2C-C.e. LIN-7, from 1 to 10 μM each, by CD. As shown in Fig. 5*D*, we observe a trend of increasing stability with increasing concentration, with an overall change in T_m from ~30 to ~37 °C over the range we measured. In further support of this model, we find that a construct of artificially tethered L27 domains, in which the effective concentration of each L27 monomer for its intramolecular binding partner should be very high, also shows cooperative unfolding behavior with a higher T_m of ~65 °C (data not shown).

Conclusions: L27 Domains Are a Novel Obligate Heterodimerization Unit—Together these data indicate that individual L27 domains are largely unfolded but adopt a helical structure when they interact to form a 1:1 simple heterodimer. L27 domains are therefore very different from most other modular protein-protein recognition domains used in signal transduction, as most such domains are independently folding units that can be transferred both structurally and functionally by recombination. This unusual property of L27 domains makes them similar to coiled-coil domains, which can also serve as specific homo- or hetero-oligomerization modules. Coiled-coils are largely unstructured independently but form a helical bundle when associated (36–38). Is it possible that L27 domains are related to the coiled-coil family? A region of certain LIN-7 homologs corresponding to the L27 domain has in fact been referred to as a potential coiled-coil domain (26, 27). However, we believe that it is unlikely that the L27 domain is a canonical coiled-coil. The region of LIN-7 that may be a putative coiled-coil is extremely short (15 amino acids), especially compared with the length of L27 domains (~65 residues) required for association. Further, analysis of multiple aligned L27 domain sequences shows no consistent propensity to form coiled-coil domains (according to either the COILS program or MULTICOIL analysis) (39–41). Even within the LIN-7 family, the putative coiled-coil motif is not conserved (26). Although it may be possible that some element of the L27 heterodimer adopts a coiled-coil-like structure, the L27 domain is unlikely to be a

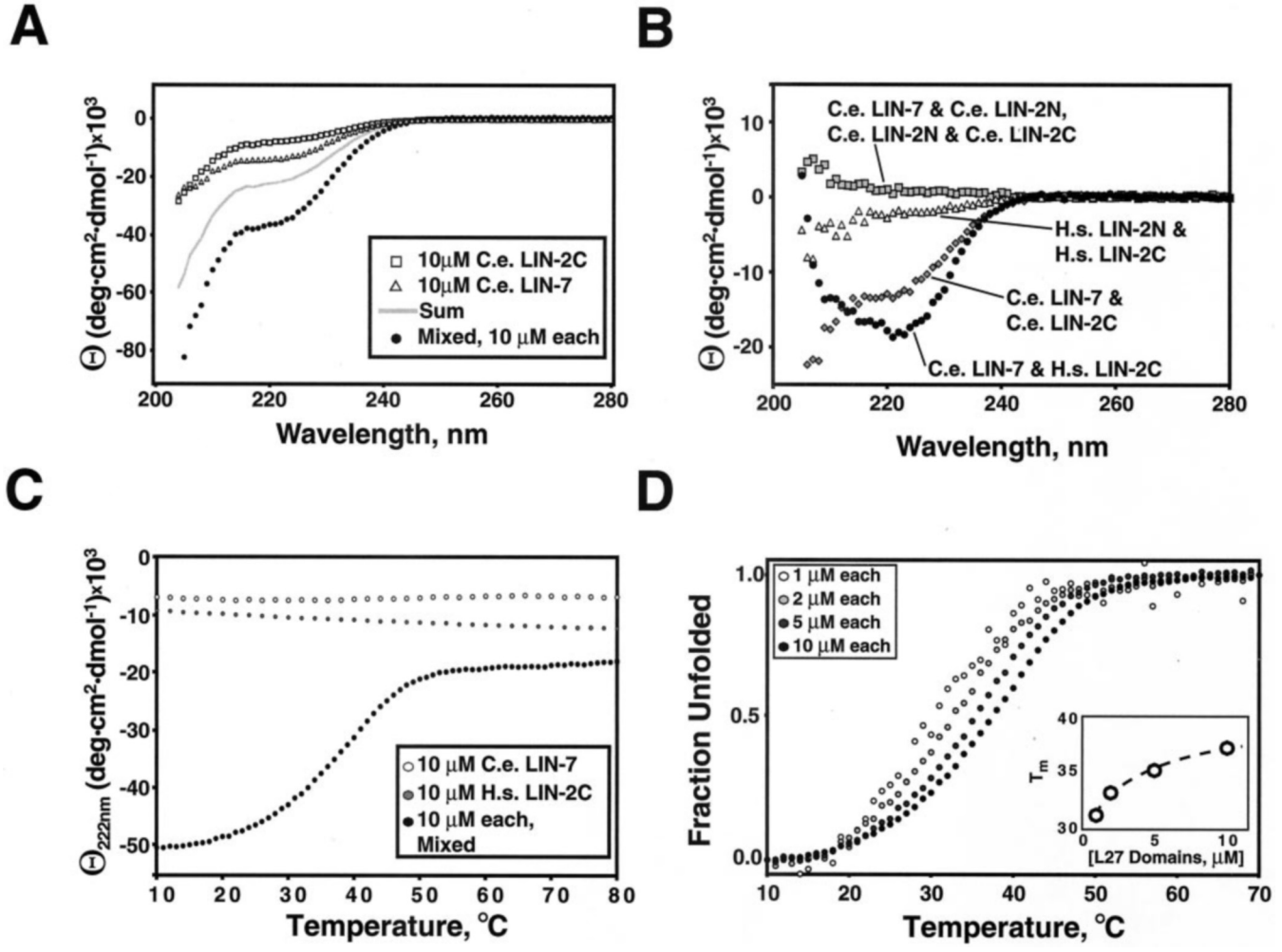

FIG. 5. **Oligomerization and folding in L27 domains are linked.** *A*, circular dichroism spectra of individual C.e. LIN-7 and C.e. LIN-2C domains (10 μM each), showing a significant change in ellipticity upon mixing of the domains (C.e. LIN-7 + C.e. LIN-2C, 10 μM each). The spectrum of the mixed L27 monomers differs significantly from the sum of individual spectra (*gray line*). *B*, difference spectra for binding and non-binding L27 pairs. The sum of CD spectra of individual monomers was subtracted from the spectra of mixed L27 monomers. Difference spectra for interacting pairs (C.e. LIN-7:C.e. LIN-2C, C.e. LIN-7:H.s. LIN-2C) show minima at 222 nm, indicative of a significant increase in α-helical content upon association. Difference spectra of non-interacting pairs (C.e. LIN-7:C.e. LIN-2N, C.e. LIN-2N:C.e. LIN-2C, H.s. LIN-2N:H.s. LIN-2C) do not show a significant deviation from zero. *C*, thermal denaturation of C.e. LIN-7, H.s. LIN-2C, and the mixed C.e. LIN-7:H.s. LIN-2C domain pair, monitoring ellipticity at 222 nm. Individual domains do not show a cooperative unfolding transition. However, mixed C.e. LIN-7 and H.s. LIN-2C show a sigmoidal curve indicative of a cooperative unfolding event. *D*, concentration dependence of stability in the C.e. LIN-7:H.s. LIN-2C L27 pair. Stoichiometric amounts of each L27 domain were mixed at 1 μM each (*white circles*), 2 μM each (*light gray circles*), 5 μM each (*dark gray circles*), and 10 μM each (*black circles*). Data were normalized to fraction unfolded; apparent noise at lower concentrations reflects the larger signal-to-noise ratio observed when working near the sensitivity limit of the CD spectrapolarimeter. A concentration dependence of temperature stability can be seen with a range of T_m from ~30 to ~37 °C (*inset*).

canonical coiled-coil. A definitive answer to this question awaits high resolution structural information for the complex. Nonetheless, it appears likely that these domains represent a novel class of obligate heterodimerization modules.

In any case, the L27 domain is one of a growing class of proteins that alone exist in an unstructured state but become structured upon functional interactions (42). These types of interactions are often found in regulatory proteins; they can be used to subtly adjust ligand affinity or can be subject to regulation via inhibitory interactions that stabilize other competing structures. It is possible that the intrinsically unstructured L27 oligomerization domains are used to regulate assembly of the LIN-2·LIN-7·LIN-10 complex, perhaps stabilizing a complex only when all of the correct binding partners are present.

Acknowledgments—We gratefully acknowledge the assistance of the following people, without whom this work would not have been possible: Alan Frankel, Chandreyee Das, Erin Cunningham, and David Agard for use of and technical assistance with CD spectroscopy, Giselle Knudsen and R. Dyche Mullins for technical assistance and advice with analytical ultracentrifugation, Cori Bargman for providing us with the *C. elegans* cDNA library, and David Julius for providing us with the *R. norvegicus* cDNA library. Peter Chien, Volker Dötsch, Giselle Knudsen, R. Dyche Mullins, Jonathan Weissman, and members of the Lim laboratory provided helpful suggestions and critical reading of the manuscript.

REFERENCES

1. Bredt, D. S. (1998) *Cell* **94,** 691–694
2. Dotti, C. G., and Simons, K. (1990) *Cell* **62,** 63–72
3. Fanning, A. S., and Anderson, J. M. (1999) *Curr. Opin. Cell Biol.* **11,** 432–439
4. Harris, B. Z., and Lim, W. A. (2001) *J. Cell Sci.* **114,** 3219–3231
5. Sheng, M., and Kim, E. (2000) *J. Cell Sci.* **113,** 1851–1856
6. Rongo, C. (2001) *Cytokine Growth Factor Rev.* **12,** 349–359
7. Craven, S. E., and Bredt, D. S. (1998) *Cell* **93,** 495–498
8. Hoskins, R., Hajnal, A. F., Harp, S. A., and Kim, S. K. (1996) *Development* **122,** 97–111
9. Kaech, S. M., Whitfield, C. W., and Kim, S. K. (1998) *Cell* **94,** 761–771
10. Simske, J. S., Kaech, S. M., Harp, S. A., and Kim, S. K. (1996) *Cell* **85,** 195–204
11. Whitfield, C. W., Bénard, C., Barnes, T., Hekimi, S., and Kim, S. K. (1999) *Mol. Biol. Cell* **10,** 2087–2100
12. Rongo, C., Whitfield, C. W., Rodal, A., Kim, S. K., and Kaplan, J. M. (1998) *Cell* **94,** 751–759
13. Butz, S., Okamoto, M., and Südhof, T. C. (1998) *Cell* **94,** 773–782
14. Cohen, A. R., Woods, D. F., Marfatia, S. M., Walther, Z., Chishti, A. H.,

Anderson, J. M., and Wood, D. F. (1998) *J. Cell Biol.* **142,** 129–138
15. Ide, N., Hirao, K., Hata, Y., Takeuchi, M., Irie, M., Yao, I., Deguchi, M., Toyoda, A., Nishioka, H., Mizoguchi, A., and Takai, Y. (1998) *Biochem. Biophys. Res. Commun.* **243,** 634–638
16. Irie, M., Hata, Y., Deguchi, M., Ide, N., Hirao, K., Yao, I., Nishioka, H., and Takai, Y. (1999) *Oncogene* **18,** 2811–2817
17. Jo, K., Derin, R., Li, M., and Bredt, D. S. (1999) *J. Neurosci.* **19,** 4189–4199
18. Tseng, T. C., Marfatia, S. M., Bryant, P. J., Pack, S., Zhuang, Z., O'Brien, J. E., Lin, L., Hanada, T., and Chishti, A. H. (2001) *Biochim. Biophys. Acta* **1518,** 249–259
19. Hata, Y., Butz, S., and Sudhof, T. C. (1996) *J. Neurosci.* **16,** 2488–2494
20. Kamberov, E., Makarova, O., Roh, M., Liu, A., Karnak, D., Straight, S., and Margolis, B. (2000) *J. Biol. Chem.* **275,** 11425–11431
21. Biederer, T., and Sudhof, T. C. (2000) *J. Biol. Chem.* **275,** 39803–39806
22. Borg, J. P., Straight, S. W., Kaech, S. M., de Taddéo-Borg, M., Kroon, D. E., Karnak, D., Turner, R. S., Kim, S. K., and Margolis, B. (1998) *J. Biol. Chem.* **273,** 31633–31636
23. Borg, J. P., Lopez-Figueroa, M. O., de Taddeo-Borg, M., Kroon, D. E., Turner, R. S., Watson, S. J., and Margolis, B. (1999) *J. Neurosci.* **19,** 1307–1316
24. Setou, M., Nakagawa, T., Seog, D. H., and Hirokawa, N. (2000) *Science* **288,** 1796–1802
25. Straight, S. W., Karnak, D., Borg, J. P., Kamberov, E., Dare, H., Margolis, B., and Wade, J. B. (2000) *Am. J. Physiol.* **278,** F464–F475
26. Olsen, O., Liu, H., Wade, J. B., Merot, J., and Welling, P. A. (2002) *Am. J. Physiol.* **282,** C183–C195
27. Straight, S., Chen, L., Karnak, D., and Margolis, B. (2001) *Mol. Biol. Cell* **12,** 1329–1340
28. Doerks, T., Bork, P., Kamberov, E., Makarova, O., Muecke, S., and Margolis, B. (2000) *Trends Biochem. Sci* **25**, 317–318
29. Lee, S., Fan, S., Makarova, O., Straight, S., and Margolis, B. (2002) *Mol. Cell. Biol.* **22,** 1778–1791
30. Roh, M. H., Makarova, O., Liu, C. J., Shin, Lee, S., Laurinec, S., Goyal, M., Wiggins, R., and Margolis, B. (2002) *J. Cell Biol.* **157,** 161–172
31. Hillier, B. J., Christopherson, K. S., Prehoda, K. E., Bredt, D. S., and Lim, W. A. (1999) *Science* **284,** 812–815
32. Harris, B. Z., Hillier, B. J., and Lim, W. A. (2001) *Biochemistry* **40,** 5921–5930
33. Nguyen, J. T., Turck, C. W., Cohen, F. E., Zuckermann, R. N., and Lim, W. A. (1998) *Science* **282,** 2088–2092
34. Mullins, R. D., Kelleher, J. F., Xu, J., and Pollard, T. D. (1998) *Mol. Biol. Cell* **9,** 841–852
35. Bubb, M. R., Lewis, M. S., and Korn, E. D. (1994) *J. Biol. Chem.* **269,** 25587–25591
36. Hurst, H. C. (1995) *Protein Profile* **2,** 101–168
37. Thompson, K. S., Vinson, C. R., and Freire, E. (1993) *Biochemistry* **32,** 5491–5496
38. Alber, T. (1992) *Curr. Opin. Genet. Dev.* **2,** 205–210
39. Schultz, J., Copley, R. R., Doerks, T., Ponting, C. P., and Bork, P. (2000) *Nucleic Acids Res.* **28,** 231–234
40. Lupas, A., Van Dyke, M., and Stock, J. (1991) *Science* **252,** 1162–1164
41. Wolf, E., Kim, P. S., and Berger, B. (1997) *Protein Sci.* **6,** 1179–1189
42. Dyson, H. J., and Wright, P. E. (2002) *Curr. Opin. Struct. Biol.* **12,** 54–60
43. Schultz, J., Milpetz, F., Bork, P., and Ponting, C. P. (1998) *Proc. Natl. Acad. Sci. U. S. A.* **95,** 5857–5864